

## Microscale Generation of Cardiospheres Promotes Robust Enrichment of Cardiomyocytes Derived from Human Pluripotent Stem Cells

Doan C. Nguyen,<sup>1,5</sup> Tracy A. Hookway,<sup>2,5</sup> Qingling Wu,<sup>1,2</sup> Rajneesh Jha,<sup>1</sup> Marcela K. Preininger,<sup>1,2</sup> Xuemin Chen,<sup>1</sup> Charles A. Easley,<sup>3</sup> Paul Spearman,<sup>1</sup> Shriprasad R. Deshpande,<sup>1</sup> Kevin Maher,<sup>1</sup> Mary B. Wagner,<sup>1</sup> Todd C. McDevitt,<sup>2,4,\*</sup> and Chunhui Xu<sup>1,4,\*</sup>

<sup>1</sup>Department of Pediatrics, Emory University School of Medicine and Children's Healthcare of Atlanta, Atlanta, GA 30322, USA

<sup>2</sup>Wallace H. Coulter Department of Biomedical Engineering, Georgia Institute of Technology and Emory University, Atlanta, GA 30332, USA

<sup>3</sup>Department of Cell Biology, Emory University School of Medicine, Atlanta, GA 30322, USA

<sup>4</sup>Parker H. Petit Institute for Bioengineering and Bioscience, Georgia Institute of Technology, Atlanta, GA 30332, USA

<sup>5</sup>Co-first author

\*Correspondence: [todd.mcdevitt@bme.gatech.edu](mailto:todd.mcdevitt@bme.gatech.edu) (T.C.M.), [chunhui.xu@emory.edu](mailto:chunhui.xu@emory.edu) (C.X.)

<http://dx.doi.org/10.1016/j.stemcr.2014.06.002>

This is an open access article under the CC BY-NC-ND license (<http://creativecommons.org/licenses/by-nc-nd/3.0/>).

### SUMMARY

Cardiomyocytes derived from human pluripotent stem cells (hPSCs) are a promising cell source for regenerative medicine, disease modeling, and drug discovery, all of which require enriched cardiomyocytes, ideally ones with mature phenotypes. However, current methods are typically performed in 2D environments that produce immature cardiomyocytes within heterogeneous populations. Here, we generated 3D aggregates of cardiomyocytes (cardiospheres) from 2D differentiation cultures of hPSCs using microscale technology and rotary orbital suspension culture. Nearly 100% of the cardiospheres showed spontaneous contractility and synchronous intracellular calcium transients. Strikingly, from starting heterogeneous populations containing ~10%–40% cardiomyocytes, the cell population within the generated cardiospheres featured ~80%–100% cardiomyocytes, corresponding to an enrichment factor of up to 7-fold. Furthermore, cardiomyocytes from cardiospheres exhibited enhanced structural maturation in comparison with those from a parallel 2D culture. Thus, generation of cardiospheres represents a simple and robust method for enrichment of cardiomyocytes in microtissues that have the potential use in regenerative medicine as well as other applications.

### INTRODUCTION

Cardiomyocytes (CMs) derived from human pluripotent stem cells (hPSCs) have been found in preclinical studies to prevent the progression of heart failure and function as a biological pacemaker, and therefore are a promising cell source for regenerative medicine to treat cardiovascular diseases (Burridge et al., 2012; Maher and Xu, 2013; Mummery et al., 2012). Extensive engraftment of hPSC-CMs and electromechanical coupling of these cells with the host have been demonstrated in a nonhuman primate model (Chong et al., 2014). An area of great interest to the field of stem cell research is engineering tissue constructs from hPSC-CMs, with the aim of providing better transplantable constructs for regenerative cardiac therapy as well as in vitro models to study human cardiac development, health, and disease. Many current approaches often require a great deal of effort to prepare enriched CMs from differentiation cultures; for example, CMs can be enriched by a mitochondrial dye (Hattori et al., 2010) or metabolic selection (Tohyama et al., 2013) and then aggregated, or by fluorescence-activated cell sorting based on surface markers for the generation of tissue patches (Zhang et al., 2013). Genetically modified hPSCs have also been used to select cardiac progenitors or CMs for the production of tissue-engineered cardiac

constructs (Emmert et al., 2013; Thavandiran et al., 2013).

Several strategies to generate tissue-engineered cardiac constructs have been considered, including the self-assembly of 3D cell aggregates. Such aggregates offer several advantages and can be easily generated by forced aggregation and maintained in a rotary orbital suspension culture (Kinney et al., 2011). Microscale technologies allow for the generation of size-controlled 3D multicellular aggregates (Khademhosseini et al., 2006) that can promote cell-cell and cell-matrix interactions analogous to those observed among cells in vivo, which cannot be achieved in traditional 2D cultures. Furthermore, in contrast to macro-tissue constructs, microtissue constructs can obviate limitations of oxygen and nutrient transport, do not require additional matrix or scaffold materials, and are suitable for scale-up suspension production, and thus represent a robust method for cardiac tissue engineering (Kinney et al., 2014). Therefore, we produced and characterized scaffold-free 3D cardiospheres from 2D differentiation cultures of hPSCs using microscale technologies. The combined technique of forced aggregation and 3D suspension culture is capable of robustly and rapidly enriching CMs from heterogeneous differentiation cultures, and also promotes enhanced structural maturation of CMs compared with parallel 2D cultures.



## RESULTS

### Derivation of Human Induced PSC Lines and CM Differentiation

We generated 3D cardiospheres using two human induced pluripotent stem cell (iPSC) lines, 903-19 and 903-20, derived from human dermal fibroblasts (Figure S1 available online); the IMR90 iPSC line (Yu et al., 2007); and the H7 human embryonic stem cell (hESC) line (Thomson et al., 1998). The generated iPSCs expressed PSC markers and generated cell types of all three germ layers (Figure S1), indicating that the 903-19 and 903-20 lines were bona fide PSC lines that might be used for subsequent CM differentiation.

To induce CM differentiation in 2D cultures of the four hPSC lines, the cells were sequentially treated with activin A and BMP4 (Laflamme et al., 2007) or small molecules targeting the Wnt pathway (Lian et al., 2012). In general, spontaneously beating clusters were first observed between days 7 and 9, and gradually increased in number over time. By day 14, cells across large regions of the cultures were strongly contracting (Movie S1) and continued to beat vigorously until they were harvested.

### Generation of Uniform Cardiospheres via Microscale Forced Aggregation and Suspension Culture

To produce cardiospheres, 2D differentiation cultures were dissociated and seeded into microwells (Figure 1A). After 24 hr, cell aggregates were transferred to suspension culture and maintained for 7 days. The cells consistently aggregated to form 3D cardiospheres regardless of the initial CM differentiation efficiency (~10%–40%). After 2 days and for the duration of the suspension culture, ~100% of the resulting cardiospheres exhibited spontaneous beating (Movie S2). The cardiospheres maintained their starting size for the entire suspension culture period (Figures 1B and 1C). Histological analysis indicated that the cardiospheres consisted of densely packed cells that were entrapped with relatively little collagen and glycosaminoglycans and lacked visible necrotic centers (Figure 1D), in contrast to the necrotic regions that are often observed in large (>600  $\mu\text{m}$  in diameter) multicellular aggregates of PSCs (Gerecht-Nir et al., 2004).

We next determined whether the cardiospheres had appropriate calcium-handling properties. When incubated with a calcium indicator dye, Fluo-4, all of the cardiospheres showed calcium impulses (Movie S3). Optical recordings of intracellular calcium transients by line scans reflected appropriate cyclic calcium handling (Figure 1E). The average spontaneous beating frequency for these cells was 0.49 Hz, which was in the range reported in the literature for functional hESC-CMs (Lundy et al., 2013), and the amplitude was also consistent with what has been measured in human cardiac cells (Wagner et al., 2005).

Other measured parameters, including times to 50% peak and to 50% decay, were also representative of a cardiac-type phenotype. In addition, increased spontaneous beating rates were observed when cells were treated with isoproterenol, a  $\beta$ -adrenergic agonist, indicating an appropriate pharmacological response (Figure 1F).

Altogether, these results suggest that the combination of microscale forced aggregation and suspension culture enables the reliable generation of cardiospheres that retain appropriate calcium handling properties and pharmacological response.

### Robust Enrichment of CMs via Cardiosphere Formation

The gross distribution of CMs within cardiospheres was examined by whole-mount staining. Sarcomeric  $\alpha$ -actinin<sup>+</sup> cells were observed throughout cardiospheres, and punctate connexin 43 staining was seen between the cells within the constructs (Figure 2A). These staining patterns indicated that the majority of the cells in the aggregates were CMs. To further evaluate whether enrichment of CMs occurred in cardiospheres, the proportion of CMs in dissociated cardiospheres was compared with that in parallel 2D cultures by immunocytochemical analysis of  $\alpha$ -actinin. Staining of cells from cardiospheres indicated that  $\alpha$ -actinin<sup>+</sup> cells were abundantly present, with only rare instances of unstained cells (Figure 2B, bottom). In contrast, the majority of cells in 2D cultures lacked  $\alpha$ -actinin expression (Figure 2B, top). These results demonstrated that CMs had been greatly enriched from 2D cultures.

To quantify the enrichment efficiency, flow-cytometric analysis was used to determine the percentages of  $\alpha$ -actinin<sup>+</sup> cells in cardiospheres and parallel 2D cultures. As depicted in Figures 2C and 2D, the percentage of  $\alpha$ -actinin<sup>+</sup> cells from 3D cultures was enriched to ~90% from ~40%, and to ~80% from ~10%, respectively, from parallel monolayer cultures, translating to an enrichment factor of ~2- to 7-fold. This finding indicated that cardiosphere culture enabled robust enrichment of hPSC-CMs, irrespective of the initial differentiation efficiency of the starting population.

### Role of Cell Aggregation in CM Enrichment

To understand the process of CM enrichment and determine when the enrichment primarily occurred, we analyzed the CM purity of cardiospheres and parallel 2D cultures at several time points: before (day 14) and immediately after aggregation (day 14+1) and after 3 or 7 days in suspension culture (day 14+3 and day 14+7, respectively). An input cell population from a 2D culture of H7 cells containing ~30%  $\alpha$ -actinin<sup>+</sup> cells at day 14 was forced to aggregate into 3D cardiospheres. Compared with parallel 2D

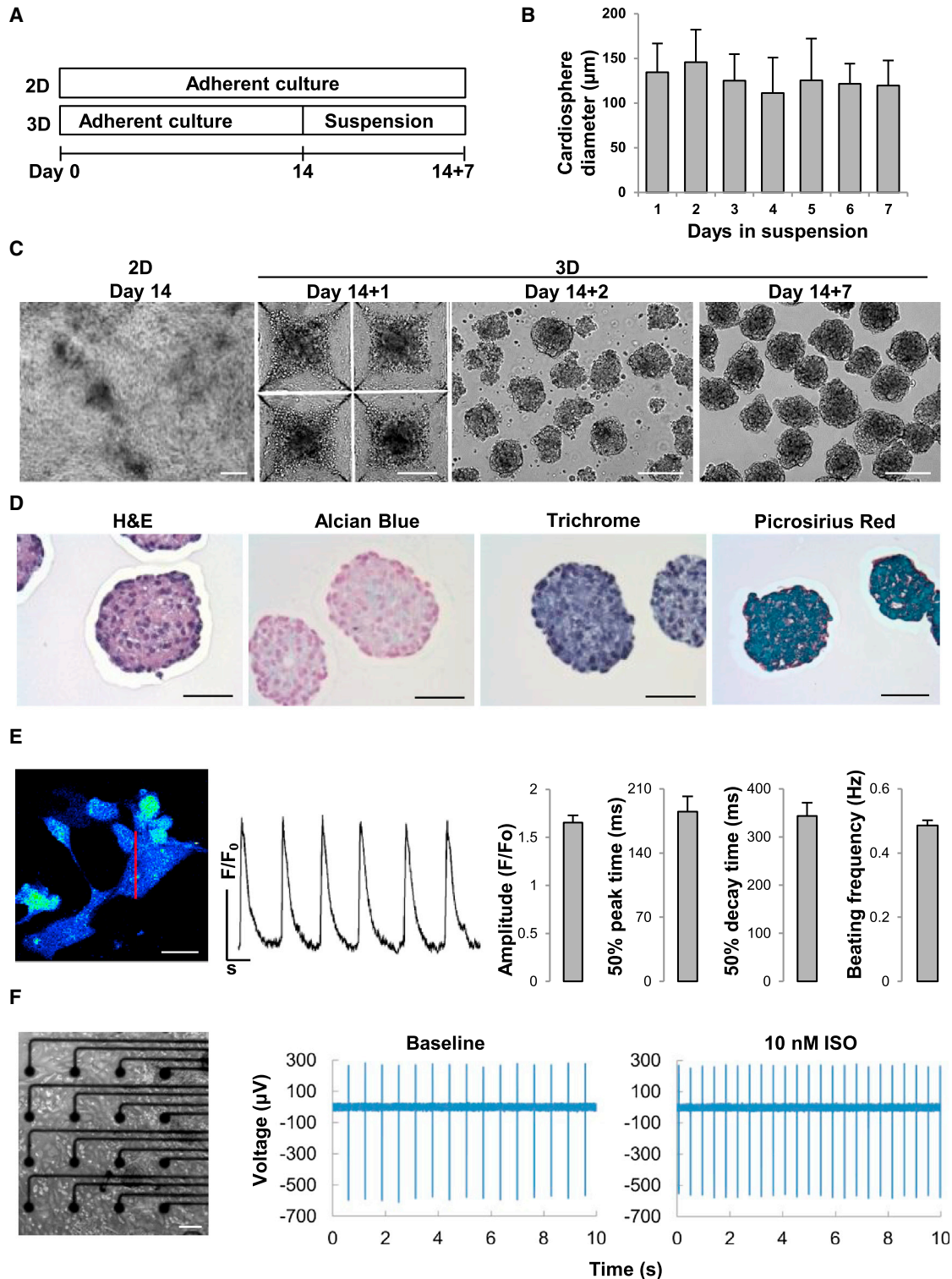


**Figure 1. CM Differentiation on Monolayers and Engineering of 3D Cardiospheres**

(A) Schematic outlining the procedures used to differentiate hPSCs to CMs in 2D culture and to engineer 3D cardiospheres from 2D cultures. (B) Size distribution (mean ± SD; n = 11–56 cardiospheres for each time point) of cardiospheres during suspension culture. (C) Phase-contrast images of CMs generated on monolayers on day 14 postinduction (2D; left), cells 1 day after seeding in microwells (3D; day 14+1), and cardiospheres on day 2 (3D; day 14+2) and day 7 (3D; day 14+7) in suspension. Scale bars represent 200 μm. (legend continued on next page)



controls, which maintained similar levels of purity during 1 week of adherent culture, the CMs in cardiospheres increased to ~60% 1 day after initiation of cell aggregation (day 14+1), and further increased to ~90% by 3 and 7 days in suspension (days 14+3 and 14+7, respectively; [Figure 3A](#)). Therefore, CM enrichment occurred early after initial aggregation and increased further during the subsequent suspension culture phase.

Since enrichment of CMs occurred 1 day after initiation of aggregation, this process was monitored more closely. An input 2D culture containing ~20%  $\alpha$ -actinin<sup>+</sup> cells with ~90% viability (measured by trypan blue exclusion) was used to form cardiospheres ([Figure S2](#)). After 24 hr, a subset of the cells incorporated into cardiospheres while the rest of the cells remained as single cells or small clusters in the supernatant. With input cells at 1,500 cells/microwell, each cardiosphere contained ~600 cells after 1 day of cardiosphere formation, suggesting that selective cell aggregation occurred during cardiosphere formation.

To evaluate the fate of noncardiac cells, we collected both cells in the supernatant fraction (which are typically removed during medium changes) and cardiospheres, and examined them for cell viability and purity of CMs. Cells in the supernatant were mostly single cells with a poor cell viability (~10%). In contrast, the viability of the cells from dissociated 3D cardiospheres was ~90%. When cells from the supernatant were replated, a majority of the cells remained unattached and the cells that did survive were mostly negative for  $\alpha$ -actinin. In contrast, cells from cardiospheres attached well and the percentage of  $\alpha$ -actinin<sup>+</sup> cells increased from ~20% in the 2D culture to ~60% in cardiospheres ([Figure S2](#)). Cell counting indicated that ~20% of the initial input non-CMs were recovered in the cardiospheres, suggesting that the majority of non-CMs were dead and remained in the supernatant. Addition of a ROCK inhibitor during cardiosphere formation did not affect viability or CM enrichment ([Figure S2](#)). The dramatic difference in cell viability between cardiospheres and cells in the supernatant was confirmed by Annexin V and propidium iodide (PI) staining ([Figure 3B](#)). Cardiospheres consisted of ~90% Annexin V<sup>-</sup>/PI<sup>-</sup> (live) cells; in contrast, cells in the supernatant consisted of only ~20% live cells. These

results suggest that CMs can preferentially survive and form cardiospheres, whereas the majority of the unincorporated non-CMs do not.

To examine whether the size of the cardiospheres affected enrichment, we formed aggregates of 500, 1,000, or 1,500 input cells/microwell by varying the density of the initial cell suspension ([Figure S3A](#)). The input of 500 cells/microwell yielded noticeably smaller aggregates compared with the input of 1,000 or 1,500 cells/microwell. We found that ~97%–100% cells from cardiospheres in all three conditions were positive for  $\alpha$ -actinin, whereas only ~14% of the cells from the 2D culture were  $\alpha$ -actinin<sup>+</sup>, suggesting that different seeding densities did not affect the overall enrichment of CMs, but did yield cardiospheres of different sizes ([Figure S3B](#)).

Next, we examined whether the proliferation of CMs or conversion from non-CMs (progenitors) into CMs contributed to CM enrichment. Cells from a 2D culture and cardiospheres were costained with antibodies against pH3 (a marker for cells in the proliferative M phase),  $\alpha$ -actinin, or NKX2-5 with  $\alpha$ -actinin. Only ~2%–4% of pH3<sup>+</sup>/ $\alpha$ -actinin<sup>+</sup> cells were detected within the  $\alpha$ -actinin<sup>+</sup> cells, and ~1%–4% NKX2-5<sup>+</sup>/ $\alpha$ -actinin<sup>-</sup> cardiac progenitors were detected, suggesting that proliferation of CMs or conversion from progenitors into CMs was unlikely a major contributor to the enrichment of CMs ([Figure S3C](#)). Collectively, these observations suggest that selective cell survival and homophilic adhesion of CMs result in aggregation to form cardiospheres with significant CM enrichment.

To investigate the involvement of specific cell adhesion molecules (N-cadherin and neural cell adhesion molecule-1 [NCAM-1]) in CM aggregation, we incubated dissociated 2D differentiated cultures with antibodies targeting N-cadherin or NCAM-1. At 0 hr, cells in all conditions remained mostly as dissociated single cells. After 4 hr of incubation, we observed large cell aggregates at the center of all wells except those containing perturbing antibodies against NCAM-1, where small cell clusters and single cells were seen throughout the wells. When transferred to flat wells, these aggregates and small clusters maintained their general appearance ([Figure 3C](#)). These observations

(D) Histological analysis of cardiospheres after 7 days in suspension culture. Scale bars represent 50  $\mu$ m.

(E) Calcium transient recordings in live CMs from cardiosphere outgrowths. Left, 2D scans of a cardiosphere outgrowth loaded with Fluo-4, where increasing calcium is indicated by the change in color from dark blue to light green. The red line indicates the location at which the line scan was recorded. Scale bar represents 20  $\mu$ m. Middle, average calcium intensity along the line scan, with all transients demonstrating cyclic calcium handling. The fluorescence intensity for all recordings is normalized to the baseline measured at time 0 ( $F_0$ ). Right, summary of the characteristics of calcium transients from cardiosphere outgrowths (mean  $\pm$  SE; line scans of  $n = 18$  cardiosphere outgrowths).

(F) Pharmacological response of CMs from cardiospheres. The morphology of dissociated cardiospheres in a multielectrode array (MEA) chamber and representative MEA recordings before and after incubation with the  $\beta$ -adrenergic agonist isoproterenol (10 mM) are shown. Note that the beating rate increased upon treatment with isoproterenol. Scale bar represents 100  $\mu$ m.

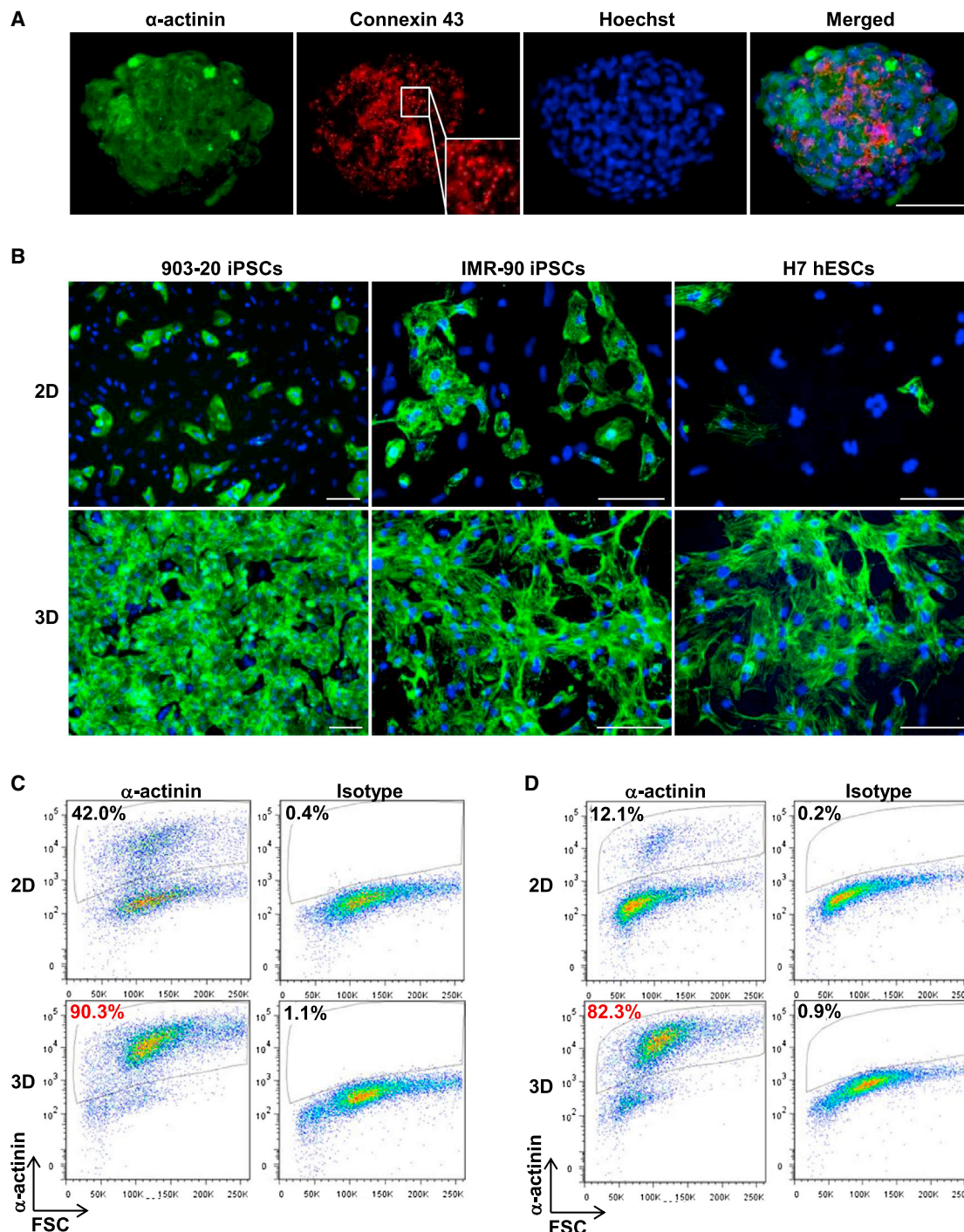


**Figure 2. Enrichment of hPSC-CMs via 3D Cardiosphere Culture**

(A) Whole-mount staining of 3D cardiospheres for sarcomeric  $\alpha$ -actinin and connexin 43. Scale bar represents 50  $\mu$ m.  
(B) Immunostaining for  $\alpha$ -actinin of cells harvested from day 21 monolayer cultures (2D; top) and day 7 cardiospheres (3D; bottom) (day 14+7). Dissociated cells from cultures generated from three hPSC lines were immunostained for sarcomeric  $\alpha$ -actinin (green) and counterstained for nuclei with DAPI (blue). Scale bars represent 50  $\mu$ m. Note that  $\alpha$ -actinin staining is present throughout the field, with rare occurrences of unstained cells in the samples from 3D cardiospheres.

(legend continued on next page)



implicate NCAM-1 as a likely mediator of CM aggregation into cardiospheres. We next examined whether neuroectoderm cells (which can express NCAM-1) were present in the input 2D cells and 3D cells. SOX2, a stem cell marker that persists in neuroectoderm (Freund et al., 2008), was undetectable in both 2D and 3D cultures, indicating a lack of neuroectoderm cells in the differentiation population. These results suggest that in the absence of neuroectoderm, CMs aggregation is mediated (at least in part) by NCAM-1.

### Structural Characteristics and Modulation of Structural Maturation of CMs via Cardiosphere Formation

To examine the microstructure of CMs in cardiospheres, we stained dissociated and replated cardiospheres with cardiac markers, including sarcomeric myosin heavy chain (sMHC),  $\alpha$ -actinin, NKX2-5, and cardiac troponin I (cTnI). As shown in Figure 4A, these cells were positive for all of these markers and also featured clear muscle striations when observed under high magnification, suggestive of their bona fide CM status. Next, given the enhanced cell-cell interactions in cardiospheres, we investigated the possible effect of the suspension cultures on CM structural maturity. For this purpose, we compared the z-line sarcomere organization and morphology of CMs that originated from cardiospheres and 2D cultures. More than 200 2D and 3D  $\alpha$ -actinin<sup>+</sup> CMs were “scored” for their relative levels of z-line sarcomere organization; as such, a cell that received a higher score represented a greater level of sarcomeric structures (Figure 4B). Compared with CMs from 2D cultures, 4.4-fold more cells from 3D cardiospheres exhibited higher levels of sarcomeric striations (level 4 cells), and 1.8- to 5.1-fold fewer cells from 3D cultures showed a morphology of levels 1–3 (Figure 4C). As shown in Figure S4, the sarcomere lengths of the level 4 cells from 3D cultures were significantly higher than those of the level 4 cells from 2D cultures. The length-to-width ratios of  $\alpha$ -actinin<sup>+</sup> cells in 3D cells were also significantly higher than those in 2D cells, although no significant difference was observed for cell area and cell perimeter (Figure S4). These data suggest that cardiosphere cultures promote several features of structural maturation in hPSC-CMs.

## DISCUSSION

Overall, we show that combination of forced aggregation and suspension culture enables the reliable generation

of cardiospheres with spontaneous contractility. Strikingly, these cardiospheres contain highly enriched (up to ~100%) CMs that retain expected functional characteristics. The enrichment is particularly robust and efficient irrespective of the starting population, even when cultures contain as little as ~10% CMs. Furthermore, CMs within cardiospheres display enhanced sarcomeric structural maturation compared with those from parallel monolayer cultures. Thus, the use of cardiospheres represents a unique, simple, and straightforward method for the enrichment of CMs. Our findings highlight advantages conferred by 3D tissue engineering of CMs derived from hPSCs.

Enriched CMs are highly desirable for research and translational applications such as drug discovery and cell therapy, as well as mechanistic characterization of inherited cardiac diseases with iPSC-CMs; for example, gene-expression profiling between patient- and unaffected control-specific CMs could be confounded by low CM purity in differentiation cultures. Although efficient CM differentiation methods have been reported (Lian et al., 2012; Zhang et al., 2012), in many cases there remain large variations in CM purity in differentiation cultures, as indeed we experienced in this study even with the well-characterized H7 hESC line. Whereas several techniques allow for the enrichment of CMs from heterogeneous differentiation cultures, such methods nevertheless exist with one or more caveats, such as complex and lengthy procedures, low-to-moderate efficiency, genotoxicity, and/or production of CMs that are labeled with antibodies, dyes, or magnetic beads (BurrIDGE et al., 2012; Xu, 2012). The cardiosphere-mediated enrichment method reported here is simple to perform, is highly efficient, does not require genetic modification, and yields highly enriched CM populations free of any antibodies or dyes. Added benefits of the 3D cardiospheres include potential to overcome challenges of low rates of cell retention following transplantation of dissociated cells and to be directly used for high-throughput in vitro assays in drug discovery.

CM enrichment in cardiospheres is apparently mediated via selective cell survival and homophilic association. NCAM-1 is a cell-surface glycoprotein and calcium-independent adhesion protein that is expressed in developing hearts and other tissues, modulates cell-cell interaction during development (Watanabe, 1998), and was previously found to be highly expressed on hESC-CMs (Xu et al., 2006). This study demonstrates that NCAM-1 plays a functional role in the aggregation of hPSC-CMs. The enrichment of CMs in cardiospheres is likely facilitated

(C) Quantification of CM purity by flow-cytometric analysis for  $\alpha$ -actinin on cells derived from 903-20 iPSCs. Numbers indicate the percentage of cells positive for  $\alpha$ -actinin (left) or the matching negative isotype control (isotype; right).

(D) Same as (C) except that the 903-20 iPSC line is shown at a later passage. More than  $1 \times 10^5$  live cells (EMA-negative events) were analyzed in all flow-cytometric analyses.

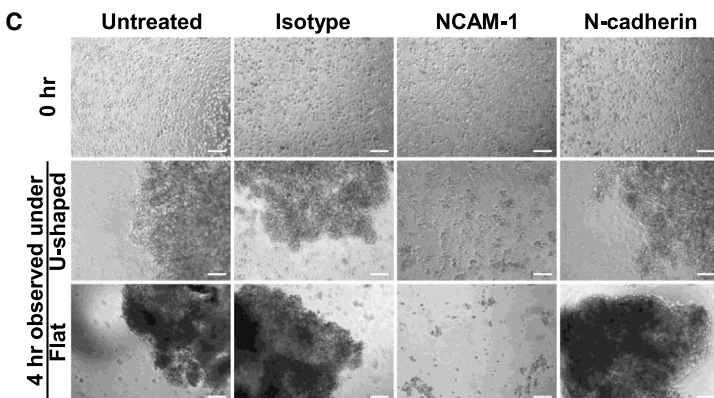
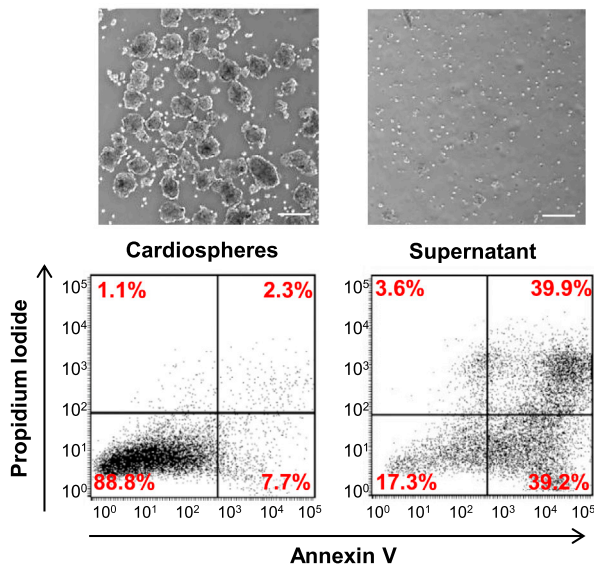
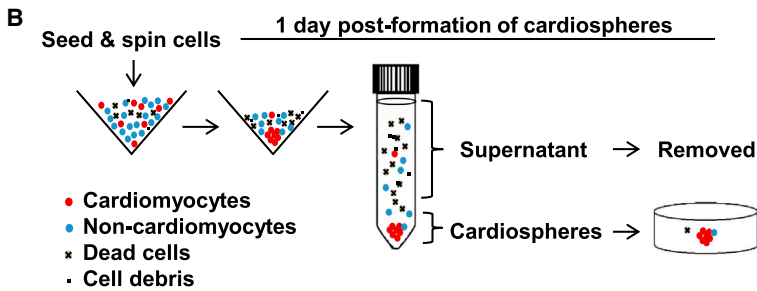
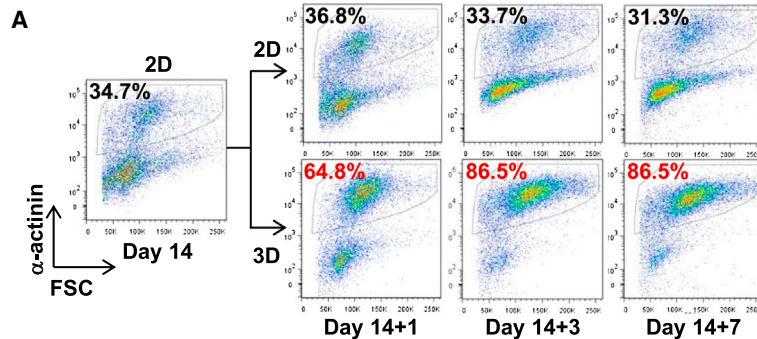


**Figure 3. Role of Cell Aggregation in CM Enrichment**

(A) Flow-cytometric analysis of  $\alpha$ -actinin in H7 2D cultures and 3D cardiospheres at several time points. The purity of CMs was analyzed at day 14, 1 day after initiation of cardiospheres (day 14+1), and after 3 and 7 days in suspension (day 14+3 and day 14+7, respectively). 2D control cultures were analyzed at the same time points. Note that enrichment of CMs was observed soon after initiation of cell aggregation and further in suspension cultures.

(B) Schematic diagram for cardiosphere formation and separation of cells from cardiospheres and supernatant, phase-contrast images, and flow-cytometric analysis of Annexin V and PI in cells from H7 cardiospheres and supernatant on day14+1. Scale bars represent 100  $\mu$ m.

(C) Cell aggregation inhibition assay. Dissociated differentiation cultures of 903-19 iPSCs were incubated in medium containing the indicated antibodies and monitored at 0 hr or 4 hr after the incubation. Note that the formation of large cell aggregates was prevented in medium containing antibodies against NCAM-1. Scale bars represent 50  $\mu$ m.

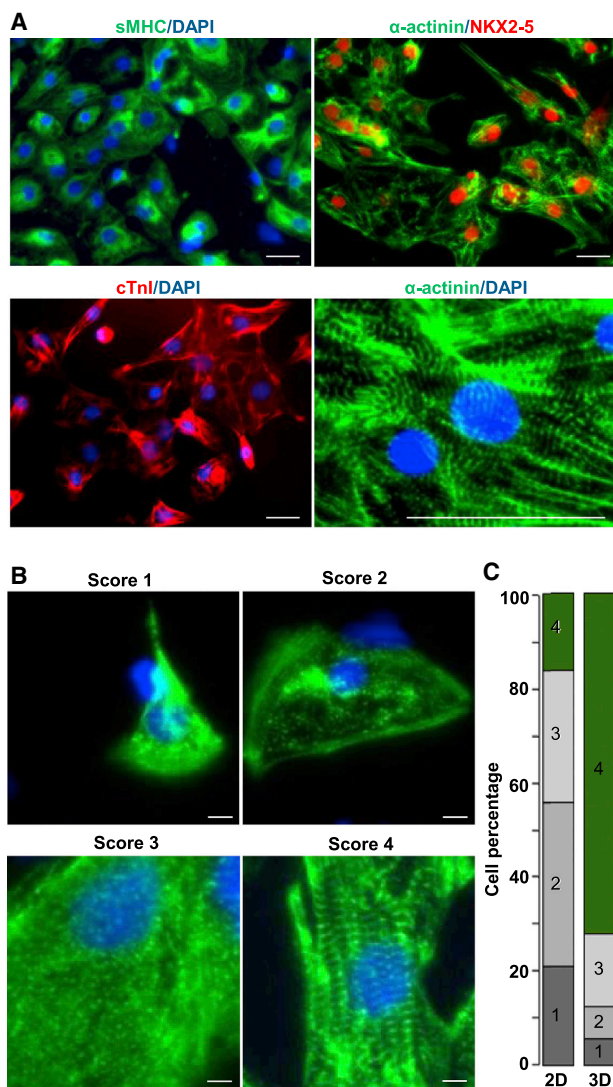


**Figure 4. Structural Analysis of CMs from 3D Cardiospheres**

(A) Immunocytochemical analysis of cardiac markers on dissociated cardiospheres derived from 903-19 iPSCs. Note that cardiac markers were present throughout the field and that a higher magnification revealed typical cardiac sarcomeric striations. Scale bars represent 50  $\mu$ m.

(B) Comparison of CM maturation between 2D culture and 3D cardiospheres derived from 903-20 iPSCs. Cardiospheres at day 14+7 and the parallel 2D culture were dissociated, replated, and stained for sarcomeric  $\alpha$ -actinin (green) and DAPI (blue). The level of sarcomeric striations was visualized from high-magnification images and given a score of 1–4. Cells that received a score of 1 stained positively for  $\alpha$ -actinin, but without clear sarcomeric striations. Cells that were scored 2, 3, or 4 had detectable sarcomeric striations at increasing levels.

(C) Percentage of cells by the scores. Note that cells from 3D cultures displayed higher numbers of cells with more clear sarcomeric striations compared with cells from 2D cultures. Scale bars represent 5  $\mu$ m.

by a lack of other cell types, such as neuroectoderm that express NCAM-1 in differentiated cultures.

The microscale cardiospheres generated herein exhibit enhanced structural maturation of CMs, suggesting a potential improvement in the utility of tissue-engineered cardiac constructs. This technology also provides a simple and effective method for the enrichment of hPSC-CMs that will be a useful cell source for regenerative therapies and can serve as simple tissue models for drug discovery and development.

## EXPERIMENTAL PROCEDURES

### Microwell Formation of Cardiospheres

To generate 3D cardiospheres, 2D differentiation cultures on days 14–23 were dissociated with 0.25% trypsin/EDTA and seeded into microwells (Aggrewell 400; StemCell Technologies) at a density of 500–1,500 cells/microwell. After 24 hr, cardiospheres were transferred to rotary orbital suspension culture (at a speed of 60–65 rpm) and maintained for up to 8 days. Upon the completion of culture, cardiospheres were harvested for subsequent characterization.

## SUPPLEMENTAL INFORMATION

Supplemental Information includes Supplemental Experimental Procedures, four figures, one table, and three movies and can be found with this article online at <http://dx.doi.org/10.1016/j.stemcr.2014.06.002>.

## AUTHOR CONTRIBUTIONS

C.X. and T.C.M. jointly conceived the study; D.C.N., T.A.H., Q.W., R.J., and M.K.P. performed research; X.C., C.A.E., P.S., S.R.D., K.M., and M.B.W. contributed new reagents and analytic tools; D.C.N., T.A.H., Q.W., R.J., M.K.P., and M.B.W. analyzed data; D.C.N. and C.X. wrote the paper; and T.A.H., M.B.W., and T.C.M. edited the paper.

## ACKNOWLEDGMENTS

We thank the staff of the Emory Children's Pediatric Research Flow Cytometry Core for training on flow cytometry. This work was supported in part by the Emory Children's Center (C.X.); the Clinical and Translational Sciences Award Program of the National Center for Advancing Translational Sciences, NIH (PHS grant UL1TR00454 to C.X. and T.C.M.); the National Science Foundation (CBET 0939511 to T.C.M.); CASIS (GA-2014-126 to C.X.), and the NIH (R21HL118454 to C.X.). Q.W. and M.K.P. were supported by the Center for Pediatric Nanomedicine under the direction of Dr. Gang Bao.

Received: February 5, 2014

Revised: May 31, 2014

Accepted: June 2, 2014

Published: July 3, 2014





## REFERENCES

- Burridge, P.W., Keller, G., Gold, J.D., and Wu, J.C. (2012). Production of de novo cardiomyocytes: human pluripotent stem cell differentiation and direct reprogramming. *Cell Stem Cell* 10, 16–28.
- Chong, J.J., Yang, X., Don, C.W., Minami, E., Liu, Y.W., Weyers, J.J., Mahoney, W.M., Van Biber, B., Palpant, N.J., Gantz, J.A., et al. (2014). Human embryonic-stem-cell-derived cardiomyocytes regenerate non-human primate hearts. *Nature*. Published online April 30, 2014. <http://dx.doi.org/10.1038/nature13233>.
- Emmert, M.Y., Wolint, P., Wickboldt, N., Gemayel, G., Weber, B., Brokopp, C.E., Boni, A., Falk, V., Bosman, A., Jaconi, M.E., and Hoerstrup, S.P. (2013). Human stem cell-based three-dimensional microtissues for advanced cardiac cell therapies. *Biomaterials* 34, 6339–6354.
- Freund, C., Ward-van Oostwaard, D., Monshouwer-Kloots, J., van den Brink, S., van Rooijen, M., Xu, X., Zweigerdt, R., Mummery, C., and Passier, R. (2008). Insulin redirects differentiation from cardiogenic mesoderm and endoderm to neuroectoderm in differentiating human embryonic stem cells. *Stem Cells* 26, 724–733.
- Gerecht-Nir, S., Cohen, S., and Itskovitz-Eldor, J. (2004). Bioreactor cultivation enhances the efficiency of human embryoid body (hEB) formation and differentiation. *Biotechnol. Bioeng.* 86, 493–502.
- Hattori, F., Chen, H., Yamashita, H., Tohyama, S., Satoh, Y.S., Yuasa, S., Li, W., Yamakawa, H., Tanaka, T., Onitsuka, T., et al. (2010). Nongenetic method for purifying stem cell-derived cardiomyocytes. *Nat. Methods* 7, 61–66.
- Khademhosseini, A., Langer, R., Borenstein, J., and Vacanti, J.P. (2006). Microscale technologies for tissue engineering and biology. *Proc. Natl. Acad. Sci. USA* 103, 2480–2487.
- Kinney, M.A., Sargent, C.Y., and McDevitt, T.C. (2011). The multiparametric effects of hydrodynamic environments on stem cell culture. *Tissue Eng. Part B Rev.* 17, 249–262.
- Kinney, M.A., Hookway, T.A., Wang, Y., and McDevitt, T.C. (2014). Engineering three-dimensional stem cell morphogenesis for the development of tissue models and scalable regenerative therapeutics. *Ann. Biomed. Eng.* 42, 352–367.
- Laflamme, M.A., Chen, K.Y., Naumova, A.V., Muskheli, V., Fugate, J.A., Dupras, S.K., Reinecke, H., Xu, C., Hassanipour, M., Police, S., et al. (2007). Cardiomyocytes derived from human embryonic stem cells in pro-survival factors enhance function of infarcted rat hearts. *Nat. Biotechnol.* 25, 1015–1024.
- Lian, X., Hsiao, C., Wilson, G., Zhu, K., Hazeltine, L.B., Azarin, S.M., Raval, K.K., Zhang, J., Kamp, T.J., and Palecek, S.P. (2012). Robust cardiomyocyte differentiation from human pluripotent stem cells via temporal modulation of canonical Wnt signaling. *Proc. Natl. Acad. Sci. USA* 109, E1848–E1857.
- Lundy, S.D., Zhu, W.Z., Regnier, M., and Laflamme, M.A. (2013). Structural and functional maturation of cardiomyocytes derived from human pluripotent stem cells. *Stem Cells Dev.* 22, 1991–2002.
- Maher, K.O., and Xu, C. (2013). Marching towards regenerative cardiac therapy with human pluripotent stem cells. *Discov. Med.* 15, 349–356.
- Mummery, C.L., Zhang, J., Ng, E.S., Elliott, D.A., Elefanty, A.G., and Kamp, T.J. (2012). Differentiation of human embryonic stem cells and induced pluripotent stem cells to cardiomyocytes: a methods overview. *Circ. Res.* 111, 344–358.
- Thavandiran, N., Dubois, N., Mikryukov, A., Massé, S., Beca, B., Simmons, C.A., Deshpande, V.S., McGarry, J.P., Chen, C.S., Nanthakumar, K., et al. (2013). Design and formulation of functional pluripotent stem cell-derived cardiac microtissues. *Proc. Natl. Acad. Sci. USA* 110, E4698–E4707.
- Thomson, J.A., Itskovitz-Eldor, J., Shapiro, S.S., Waknitz, M.A., Swiergiel, J.J., Marshall, V.S., and Jones, J.M. (1998). Embryonic stem cell lines derived from human blastocysts. *Science* 282, 1145–1147.
- Tohyama, S., Hattori, F., Sano, M., Hishiki, T., Nagahata, Y., Matsuura, T., Hashimoto, H., Suzuki, T., Yamashita, H., Satoh, Y., et al. (2013). Distinct metabolic flow enables large-scale purification of mouse and human pluripotent stem cell-derived cardiomyocytes. *Cell Stem Cell* 12, 127–137.
- Wagner, M.B., Wang, Y., Kumar, R., Tipparaju, S.M., and Joyner, R.W. (2005). Calcium transients in infant human atrial myocytes. *Pediatr. Res.* 57, 28–34.
- Watanabe, M. (1998). The neural cell adhesion molecule and heart development: what is NCAM doing in the heart? *Basic Appl. Myol.* 8, 277–291.
- Xu, C. (2012). Differentiation and enrichment of cardiomyocytes from human pluripotent stem cells. *J. Mol. Cell. Cardiol.* 52, 1203–1212.
- Xu, C., Police, S., Hassanipour, M., and Gold, J.D. (2006). Cardiac bodies: a novel culture method for enrichment of cardiomyocytes derived from human embryonic stem cells. *Stem Cells Dev.* 15, 631–639.
- Yu, J., Vodyanik, M.A., Smuga-Otto, K., Antosiewicz-Bourget, J., Frane, J.L., Tian, S., Nie, J., Jonsdottir, G.A., Ruotti, V., Stewart, R., et al. (2007). Induced pluripotent stem cell lines derived from human somatic cells. *Science* 318, 1917–1920.
- Zhang, J., Klos, M., Wilson, G.F., Herman, A.M., Lian, X., Raval, K.K., Barron, M.R., Hou, L., Soerens, A.G., Yu, J., et al. (2012). Extracellular matrix promotes highly efficient cardiac differentiation of human pluripotent stem cells: the matrix sandwich method. *Circ. Res.* 111, 1125–1136.
- Zhang, D., Shadrin, I.Y., Lam, J., Xian, H.Q., Snodgrass, H.R., and Bursac, N. (2013). Tissue-engineered cardiac patch for advanced functional maturation of human ESC-derived cardiomyocytes. *Biomaterials* 34, 5813–5820.